J. Fluid Mech. (1967), *vol.* 27, *part* 4, *pp.* 789–813
Printed in Great Britain

An analytic approach to the method of series truncation for the supersonic blunt body problem

By HSIAO C. KAO
Northrop Corporation, Norair Division, Hawthorne, California

(Received 2 December 1965 and in revised form 13 June 1966)

A method for obtaining analytic solutions to the problem of blunt bodies in the supersonic stream of an ideal gas is presented. The solutions are written in terms of power series whose coefficients are elementary functions. These solutions are approximate, but the approximation is rational, i.e. any higher approximation can, in principle, be obtained. Some of these higher approximations have been calculated. Examples are presented for various free-stream conditions and prescribed body shapes. These are compared with results from standard numerical procedure and with available experimental measurements.

1. Introduction

Calculation of the supersonic flow past a blunt body is an interesting as well as an important problem in aerodynamics. At present, the solutions to such problems are generally obtained by numerical schemes. In spite of the many analytic approaches proposed over the past two decades, an analysis of this problem is still in demand, since severe restrictions are usually imposed in order that the resulting equations be solvable. The present study presents an analytic solution in terms of elementary functions. This analytic method shows good agreement with numerical results computed by a standard method (the marching technique) and with available experimental measurements.

In this approach the method of series truncation has been re-formulated so that the strong coupling between the truncations is removed and it becomes possible to obtain an analytic solution. In previous formulations, the higher-order terms which appear in the lower-order equations usually involve pressure, or density (or its equivalent). These higher-order terms are truncated only to reduce the number of variables so that the number of unknowns matches the number of differential equations. The magnitudes of these terms dropped in the truncation are usually as large as the magnitudes of the terms retained. However, if we use Bernoulli's equation to replace the normal momentum equation in the original system of governing equations, the higher-order terms in each truncation become the velocity components normal to the body or the shock wave. Since in hypersonic flow the velocity components normal to the body or shock are much smaller than the tangential components, the truncation of the higher-order terms can then be argued on the basis of the order of magnitude comparison. Thus, one may consider the present approach to be a more rational truncation since terms are not dropped merely to reduce the number of variables. Furthermore, if additional

terms which are of the same order as the ones dropped are to be neglected, the new system of equations can be solved analytically. It was found that at least to the third-order of approximation, which has so far been determined, solutions can always be expressed in terms of elementary functions. Since these are 'rational' approximations, any higher-order approximations can, in principle, be obtained.

Since the solution to the truncated equation is obtained in closed form, this method treats both direct and inverse problems. A direct problem is defined here as one with a prescribed body shape for which the shock shape is to be determined; while an inverse problem is one with a prescribed shock wave shape and an unknown body shape which is to be determined.

The complexity of the blunt body problem is due to the fact that near the stagnation point the flow is subsonic and has a detached shock wave as its boundary whose position is not known *a priori*. However, in the problem of any practical interest, the shock position and the shock shape are not known and are a part of the problem to be determined. Thus, a portion of the boundary conditions cannot be prescribed beforehand and must be determined simultaneously with the overall flow field. A trial-and-error procedure is inevitably needed for predicting the subsonic flow field of a given blunt body in a supersonic stream (the finite difference method, which will be briefly reviewed later, brings out this process in a different manner). The procedure in most of the existing methods is simply to repeat the solution many times until it satisfies the prescribed conditions. The situation is somewhat simpler here because of the analytic nature of the solution which is in the form of algebraic equations. These algebraic equations are, however, non-linear in general, and a trial-and-error procedure is again needed to obtain the proper roots.

Many investigators have attacked the blunt body problem in the past. A review of these works can be found in Hayes & Probstein's (1959) monograph. Subsequent to the review in that book, a number of interesting studies have been published, including the following:*

(*a*) A series truncation method was developed by Swigart (1963) and Bazzhin & Gladkov (1963). Their scheme is to expand the flow variables in a series form about the stagnation point. Substitution of the series expansions into the governing equation yields a system of ordinary differential equations which are truncated and solved by numerical integrations. Since the subsonic zone is near the stagnation point, and is thin, one would expect this method to yield sufficiently accurate results using only a few terms in the series. There are, however, an unlimited number of ways to expand the flow variables. In retrospect, Swigart's choice seems to be a rather unfortunate one, the convergence of some of his series expansions being rather slow. Modifications which provide better convergence are now available (see, for example, Conti 1964; Van Dyke 1965). In particular, Van Dyke (1965) selected an inverse problem using a paraboloidal shock wave and carefully computed the resulting flow field by four different numerical methods. The results obtained by three of these methods were found to be

* Since submission of this paper, a new edition of the monograph has been published which contains a complete and up-to-date survey of this subject.

identical to four significant figures throughout the subsonic field. He, therefore, regarded this as a standard example against which other methods are to be tested.

(*b*) By using thin shock-layer approximation, an analytic method was developed by Maslen (1964). This method predicts the flow field in the transonic region, but it has some difficulties near the stagnation point. In a recent paper Cheng & Gaitatzes (1966) presented a thorough exploration of uniform validity of the shock-layer approximation and a method analogous to Maslen's. The difficulty in the nose region was removed, and their results show good agreement with the more exact numerical results for both simple and very blunt shapes.

(*c*) A modification of the integral (Belotserkovskii) method for direct calculation of blunt body flow fields was discussed by Kao (1965). Because of numerical instability, the original Belotserkovskii's scheme is not a practical method. A transformation is introduced which transplants the singularity from the differential equations to the algebraic equations. Thus, the magnitude of the problem of the numerical instability is greatly reduced.

(*d*) A finite difference method using 'artificial viscosity' was recently applied by Bohachevsky, Rubin & Mates (1965) to the blunt body problem. The numerical scheme is essentially based on Lax's (1954) work in unsteady flow. A grid is superimposed upon the flow field. The spatial derivatives in the governing differential equations along the lines making up the grid are approximated by one-level finite difference quotients. The time-dependent difference equations are then solved numerically by proceeding in time until steady state flow is reached. The artificial viscosity was introduced to keep the numerical scheme stable. Though this method is quite approximate and sometimes gives physically unreasonable results, it has the advantage of being versatile. For instance, it has been used to tackle the blunt body non-equilibrium flow problem at angle of attack.

2. Formulation of problem

The problem that we shall consider here is that of an axisymmetric blunt body at zero incidence in uniform inviscid supersonic stream. The fluid medium is assumed to be an ideal gas with constant ratio of specific heats. A spherical polar co-ordinate system is used, and is shown in figure 1, together with the velocity components where the bar denotes a dimensional quantity. It is convenient to refer the radial distance $\bar{r}$ to the shock nose radius of curvature at the stagnation streamline, the tangential and normal velocity components $\bar{u}$ and $\bar{v}$ to the free-stream velocity $\bar{U}_\infty$, the density $\bar{\rho}$ to the free-stream density $\bar{\rho}_\infty$, the pressure $\bar{p}$ to $\bar{\rho}_\infty \bar{U}_\infty^2$, and the enthalpy $\bar{h}$ to $\bar{U}_\infty^2$. The equations of motion in dimensionless quantities (quantities without bars) are then

$$\frac{\partial}{\partial r}(\rho v r^2 \sin\theta) + \frac{\partial}{\partial \theta}(\rho u r \sin\theta) = 0, \tag{1}$$

$$v\frac{\partial u}{\partial r} + \frac{u}{r}\frac{\partial u}{\partial \theta} + \frac{uv}{r} + \frac{1}{\rho r}\frac{\partial p}{\partial \theta} = 0, \tag{2}$$

$$v\frac{\partial v}{\partial r} + \frac{u}{r}\frac{\partial v}{\partial \theta} - \frac{u^2}{r} + \frac{1}{\rho}\frac{\partial p}{\partial r} = 0, \tag{3'}$$

$$v\frac{\partial h}{\partial r}+\frac{u}{r}\frac{\partial h}{\partial \theta}-\frac{1}{\rho}\left(v\frac{\partial p}{\partial r}+\frac{u}{r}\frac{\partial p}{\partial \theta}\right)=0, \tag{4'}$$

$$p=\frac{\gamma-1}{\gamma}\rho h, \tag{5}$$

where γ is the ratio of specific heats. Equations (1)–(5) are, respectively, the equations of continuity, tangential momentum, normal momentum, energy and state. Since the differential equations and the formulation of the problem vary only slightly between the two-dimensional and rotationally symmetric cases, the former is not considered here. The reduction to it is, however, straightforward.

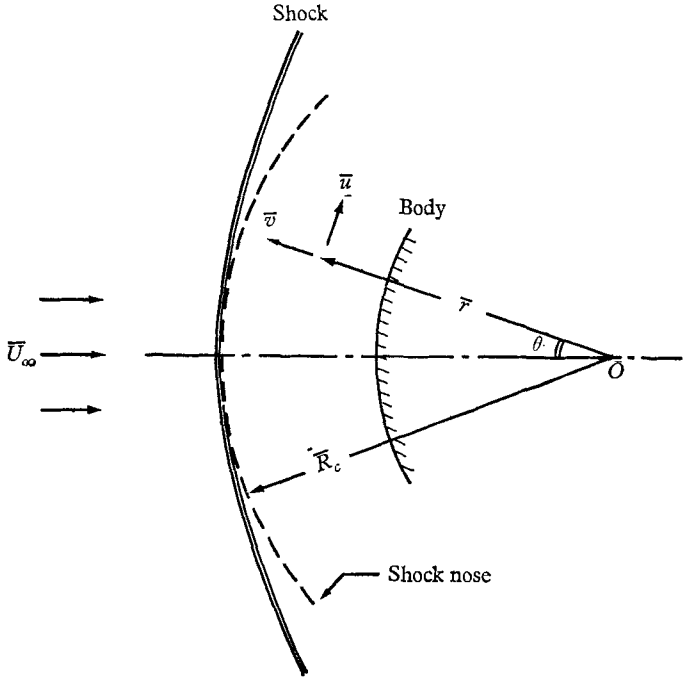

FIGURE 1. Flow configuration.

We can integrate (4') and substitute Bernoulli's equation for (3'). (The particular expansion scheme used later requires that Bernoulli's equation be substituted for the normal momentum equation rather than for the tangential momentum equation.) The system of differential equations now reduces to (1), (2),

$$(p/\rho)+k(u^2+v^2)=p_0/\rho_0, \tag{3}$$

and

$$p/\rho^\gamma=f(\psi), \tag{4}$$

where $k=(\gamma-1)/2\gamma$, the subscript 0 denotes the flow quantity evaluated at the stagnation point on the body surface, and ψ is the stream function which is defined by

$$\partial\psi/\partial r=\rho ur\sin\theta, \quad \partial\psi/\partial\theta=-\rho vr^2\sin\theta. \tag{6}$$

Although it is possible to replace the velocity components in (2) and (3) by the stream function, it is not convenient here. Hence, we still retain (1) and use the

stream function in (4) only as an intermediate parameter for expansion. The final results will be expressed as functions of the velocity components.

The equations of motion, (1)–(4), are subject to the boundary conditions at the shock and the body surface. The shock conditions are obtained from the Rankine–Hugoniot relations in terms of the shock angle ϕ and the free-stream Mach number M_∞ as follows:

$$\rho_s = [(\gamma+1)M_\infty^2 \sin^2\phi]/[(\gamma-1)M_\infty^2 \sin^2\phi + 2], \tag{7}$$

$$p_s = [2\gamma M_\infty^2 \sin^2\phi - (\gamma-1)]/[\gamma(\gamma+1)M_\infty^2], \tag{8}$$

$$m_s = \cos\phi, \tag{9}$$

$$n_s = [(\gamma-1)M_\infty^2 \sin^2\phi + 2]/[(\gamma+1)M_\infty^2 \sin^2\phi], \tag{10}$$

where the subscript s denotes the flow quantities immediately behind the shock wave, and m and n are the dimensionless velocity components tangent and normal to the shock wave respectively.

The body surface condition is simply that at the body the direction of the flow must be tangential to the body surface.

3. Method of expansion

It is a general practice to obtain solutions of linear differential equations by means of Taylor series expansions. But, when this method is applied to non-linear differential equations, it is usually impossible to find the general terms. However, if we assume that the variables in the shock layer are analytic, the method of series expansion is applicable, though the radius of convergence may not be easily estimated. In some cases the series may even be divergent. However, in solving a physical problem a divergent series may sometimes be more suitable to the purpose than a convergent one. This point is well illustrated in Van Dyke's (1964) monograph. Hence, no effort is made here to show that the following series expansion is a mathematically convergent one. (For want of a better terminology, the word 'convergence' has been used loosely to refer to better agreement with the standard numerical results. The same connotation is also implied below.) We shall demonstrate that the analytic solution agrees well with the numerical results and the available experimental measurements. Furthermore, we will also show that within the subsonic region the final result is subject only to a small modification if we calculate one more term in the series expansion. It is, nevertheless, instructive to estimate roughly the radius of convergence of the following series expansion by following the procedure in Ince's (1926) book. The radius so obtained falls approximately half way between the stagnation streamline and the sonic line.

As noted above a subsonic region exists about the stagnation point of a blunt body in a supersonic stream. The extent of this region is, however, rather limited. It is bounded by the detached shock wave, the blunt nose and the sonic line. The shock detachment distance is, in general, only a small fraction of the nose radius. This is especially true when the incoming stream is hypersonic. Moreover, the angle formed between the stagnation streamline and the sonic line is generally less than $\frac{1}{4}\pi$. Hence, we may expect that the flow variables can be expressed by

a power series in $\sin\theta$, and that a few terms of the series solution will describe the flow field satisfactorily if the shock layer is relatively thin and the backward influence is weak. This expansion has been used and substantiated by Swigart. The convergence of these series can be greatly improved if the proper variables are used. In fact, Van Dyke (1966) has shown that in one case a two-term approximation agrees closely with numerical results.

The expansion scheme used here is:

$$u(r,\theta) \sim u_1(r)\sin\theta + u_2(r)\sin^3\theta + u_3(r)\sin^5\theta + \ldots, \tag{11a}$$

$$v(r,\theta) \sim -\cos\theta[v_1(r) + v_2(r)\sin^2\theta + v_3(r)\sin^4\theta + \ldots], \tag{11b}$$

$$p(r,\theta) \sim \cos^2\theta[\pi_1(r) + \pi_2(r)\sin^2\theta + \pi_3(r)\sin^4\theta + \ldots], \tag{11c}$$

$$\rho(r,\theta) \sim \rho_1(r) + \rho_2(r)\sin^2\theta + \rho_3(r)\sin^4\theta + \ldots, \tag{11d}$$

$$\psi(r,\theta) \sim \tfrac{1}{2}[\psi_1(r)\sin^2\theta + \psi_2(r)\sin^4\theta + \psi_3(r)\sin^6\theta + \ldots], \tag{11e}$$

where

$$\psi_1 = \rho_1 v_1 r^2, \quad \psi_2 = \tfrac{1}{2}r^2(\rho_1 v_2 + \rho_2 v_1), \quad \psi_3 = \tfrac{1}{3}r^2(\rho_1 v_3 + \rho_2 v_2 + \rho_3 v_1).$$

In addition to the above series expansions of the flow variables, we must also expand the function f in (4)

$$f(\psi) \sim c + 2b\psi + 4d\psi^2 + 8e\psi^3 + \ldots, \tag{12}$$

where the coefficients b, c, d, e are constants which can be determined by using the Rankine–Hugoniot relations. The reason for the expansion of f in the form of (12) can be easily seen if we express the quantity p/ρ^γ behind the shock wave in terms of the shock angle by the Rankine–Hugoniot relations. Then we can relate the shock angle to a position on the shock wave, which in turn can be related to the stream function. This type of expression can be found in Swigart (1963). On the other hand, since (4) is the integral form of the energy equation (4′), the expanded form of (4) must be the same as that of (4′) integrated separately after substitution of the variable expansions. Substituting (11a)–(11d) into (4′) and collecting the coefficients of like powers of $\sin\theta$, we obtain the first- and higher-order equations. After we convert the velocity components in these equations to the stream functions $\psi_1, \psi_2, \ldots$ by (6) and (11e), they can be readily integrated, especially the first- and second-order ones. These integrated equations then lead to the expansion of f in the form of (12). The expansion of the pressure p, in the form given in (11c) was inspired by the hypersonic Newtonian approximation and was first suggested by Conti (1964 or 1966).

We substitute (11a)–(11e) and (12) into (1)–(4). Equating like powers of $\sin\theta$, we obtain the following system of equations:

$$r(\rho_1 v_1)' - 2\rho_1(u_1 - v_1) = 0, \tag{1a}$$

$$2\frac{p_2}{r} - \rho_1 u_1' v_1 + \rho_1 \frac{u_1}{r}(u_1 - v_1) = 0, \tag{2a}$$

$$\frac{p_1}{\rho_1} + kv_1^2 = \frac{p_0}{\rho_0}, \tag{3a}$$

$$p_1 = c\rho_1^\gamma, \tag{4a}$$

$$r(\rho_1 v_2+\rho_2 v_1)'+2(\rho_1 v_2+\rho_2 v_1)-4(\rho_1 u_2+\rho_2 u_1)=0, \tag{1b}$$

$$\frac{4p_3}{r}-\rho_1\left(u_1' v_2+u_2' v_1-\frac{4u_1 u_2}{r}+\frac{u_1 v_2+u_2 v_1}{r}\right)-\rho_2\left[u_1' v_1-\frac{u_1}{r}(u_1-v_1)\right]=0, \tag{2b}$$

$$\frac{p_2}{\rho_1}-p_1\frac{\rho_2}{\rho_1^2}+k(u_1^2-v_1^2+2v_1 v_2)=0, \tag{3b}$$

$$p_2=b\rho_1^\gamma \psi_1+\gamma p_1\frac{\rho_2}{\rho_1}, \tag{4b}$$

$$\frac{p_3}{\rho_1}-\frac{p_2\rho_2}{\rho_1^2}+\frac{p_1}{\rho_1^2}\left(\frac{\rho_2^2}{\rho_1}-\rho_3\right)+k(v_2^2+2u_1 u_2-2v_1 v_2+2v_1 v_3)=0, \tag{3c}$$

$$p_3=b\rho_1^\gamma \psi_2+b\gamma\rho_1^{\gamma-1}\rho_2\psi_1+\frac{\gamma(\gamma-1)}{2}p_1\frac{\rho_2^2}{\rho_1^2}+\gamma p_1\frac{\rho_3}{\rho_1}+d\rho_1^\gamma\psi_1^2, \tag{4c}$$

where the prime refers to differentiation with respect to r, $p_1=\pi_1$, $p_2=\pi_2-\pi_1$ and $p_3=\pi_3-\pi_2$.

This list of equations is endless. However, these ten equations are sufficient (actually too many) for obtaining the solutions for all the flow quantities with the subscript 1 and 2 (the first- and the second-order quantities) to the second iteration. Four additional equations of the next higher order are written in an appendix, and will be used to obtain the solution for the third-order quantities. Equations (1*a*) and (1*b*) are the expanded continuity equation, (2*a*) and (2*b*) the expanded tangential momentum equation, (3*a*), (3*b*) and (3*c*) the expanded Bournoulli's equation, and (4*a*), (4*b*) and (4*c*) the expanded entropy equation.

For clarity, it is necessary to distinguish between order and iteration. By order we refer to the sequence of coefficients in the power series expansions of (11*a*)–(11*e*), which is denoted by their subscripts. These coefficients are, however, some unknown functions of r, and are governed by differential equations which are to be solved by iteration. For instance, a quantity with the subscript 1 always represents a first-order quantity, but it may have many different values obtained by different levels of iteration. A higher level iteration indicates increased accuracy for the expression representing the coefficient. For instance, a third-order approximation implies that each flow variable is described by a three-term series, as in (11). If these coefficients are all in the form of the highest iteration possible within the accuracy of the third-order approximation, it is then called the 'complete' third-order approximation. As we shall see later, for each order approximation there is a maximum number of iterations for which consistent results are possible.

We now have the necessary equations for determining the first- and the second-order variables. In order to make use of the boundary conditions, they must also be expanded according to (11*a*)–(11*e*) and (12). However, since their availability is not essential for solving the above differential and algebraic equations (1*a*)–(4*c*), their presentation is deferred until later. The coefficients c, b and d in (4*a*), (4*b*) and (4*c*) are constants determinable at the shock wave by using the expanded Rankine–Hugoniot relations, provided that the shock wave shape is prescribed. If the body shape, instead of the shock wave, is prescribed, these constants will have to be determined as a part of the solution.

4. Method of analysis

The analysis is essentially based on one assumption, well known in hypersonics, that $v_1, v_2, \ldots$ are small quantities as compared with the rest of the flow quantities, such as $p_0, u_1, p_1, \ldots$, which are, in fact, of order unity. It is to be noted that $\rho_0, \rho_1, \ldots$ are not of order unity, but that $\rho_0 v_1, \rho_1 v_1, \ldots$ are. Though $v_1, v_2, \ldots$ are small quantities, their derivatives, $v_1', v_2', \ldots$ are of the same order of magnitude of $p_1, u_1, \ldots$. Notice that near the stagnation streamline the actual velocity components of u and v are small and of the same order, but it does not imply that u_1 and v_1 are of the same order, since the u and v involve the angle θ as shown in (11a) and (11b).

First, we shall consider (1a), (2a), (3a), (4a), (3b) and (4b) only. Notice that these six equations contain seven unknown variables. However, the seventh variable, v_2, which appears in the form of $2v_1 v_2$ only, can be neglected as compared with u_1^2. It is then possible, in principle, to obtain the solutions of $u_1, v_1, p_1, \rho_1, p_2$ and ρ_2.

Eliminating ρ_2 in (3b) from (4b), we have

$$p_2 = -\rho_1(\tfrac{1}{2}u_1^2 - \tfrac{1}{2}v_1^2 + v_1 v_2) - bp_1\psi_1/(\gamma-1)c. \tag{13}$$

Substituting (13) in (2a) gives simply

$$u_1' = -(u_1/r) + (v_1/r) - (2v_2/r) - 2bp_1 r/(\gamma-1)c. \tag{14}$$

Using the assumption that v_1, v_2 are an order of magnitude smaller than u_1 or p_1, we can write this equation in the form of the first iteration as

$$u_1' = -(u_1/r) - 2bp_1 r/(\gamma-1)c. \tag{14a}$$

This equation is readily integrable, provided that p_1 can be written in terms of r. Eliminating ρ_1 in (3a) from (4a), p_1 can be expanded as

$$p_1 \sim p_0 - \tfrac{1}{2}\rho_0 v_1^2 + \frac{1-2k}{8p_0}\rho_0^2 v_1^4 - \ldots. \tag{15}$$

Again, assuming that v_1 is small as compared with p_0, we can write for the first iteration

$$p_1 = p_0. \tag{15a}$$

Using the notation that $A = 4bp_0/(\gamma-1)c$, (14a) can be integrated as

$$u_1 = \tfrac{1}{2}Gr^{-1} - \tfrac{1}{6}Ar^2, \tag{16}$$

where G is an integration constant evaluated behind the shock wave. Having obtained the solution for u_1 for the first iteration, we can now determine v_1. From (1a), we have the series expansion of u_1 as

$$u_1 \sim v_1 + \tfrac{1}{2}r\left[1 - \frac{\rho_0}{\gamma p_0}v_1^2 - k\frac{\rho_0^2}{\gamma p_0^2}v_1^4 - \ldots\right]v_1'. \tag{17}$$

As above, this equation can be simplified to

$$u_1 = \tfrac{1}{2}rv_1'. \tag{17a}$$

Using (16),

$$v_1 = E - Gr^{-1} - \tfrac{1}{6}Ar^2, \tag{18}$$

where E is also an integration constant.

The calculation for the first iteration of the first-order quantities is now completed. The second iteration to be given later is essentially to improve the accuracy by including the next order terms so far neglected.

We can now immediately test the accuracy of our solutions for the first iteration. Assuming that the shock wave is spherical (to this approximation all shock waves are spherical), the integration constants can be evaluated behind the shock wave, i.e. at $r = 1$, and the standoff distances at various Mach numbers can be determined by evaluating (18), i.e. by setting $v_1 = 0$ at the body surface. Some results are shown in table 1.

		Standoff distances†		
M_∞	γ	From (18)	From (18*c*)	Spherical shocks by Van Dyke & Gordon (1959)
3	1·4	0·133	0·138	0·136
4	1·4	0·120	0·118	0·121
10	1·4	0·100	0·097	0·102
10^4	1·4	0·096	0·093	0·098

TABLE 1

In view of the approximations required to determine the first iteration, the agreement is quite remarkable. Note that (18) is a third-degree algebraic equation, which has two other roots in addition to the one related to the standoff distance. These two roots are not necessarily imaginary, however they can be rejected on the grounds that they do not agree with experimental results.

Two other approximations to (14) and (17) were found, but they were not necessarily consistent with the present argument of the first iteration. These were: (i) to add a term v_1 to (17*a*), and (ii) to add a term v_1/r to (14*a*) and a term v_1 to (17*a*). The resulting equations can also be solved exactly. The calculated value of the standoff distance is, however, less favourable.

By applying the boundary conditions immediately behind the shock wave and on the body surface, we can reduce (18) to

$$Ar^3 - (3A + 12 + 6v_{1s})r + 2A + 12 = 0, \tag{18a}$$

where v_{1s} is the value of v_1 behind the shock wave at the stagnation streamline, and is given by

$$v_{1s} = [2 + (\gamma - 1)M_\infty^2]/(\gamma + 1)M_\infty^2.$$

One root of (18*a*), which is the standoff distance, is nearly unity and can be shown to be

$$\Delta = \tfrac{1}{2}v_{1s}(1 - \tfrac{1}{8}Av_{1s} - \tfrac{1}{2}v_{1s} - \tfrac{1}{2}A^{-1}v_{1s}), \tag{18b}$$

where $\Delta = 1 - r$, the standoff distance. In this approximation, terms involving Δ^3, v_{1s}^3, etc. are neglected. Substituting the expressions for v_{1s} and A into (18*b*)

† All the dimensionless standoff distances in tables 1–4 are referred to the shock radius of curvature, $\bar{R}_c$.

and carrying out some further simplifications, we find an explicit formula for the standoff distance in terms of γ and M_∞

$$\Delta = \frac{\gamma-1}{4(\gamma+1)^2}\left[\gamma+3+p_{0t}+\frac{(\gamma-1)^2}{4p_{0t}}\right]+\frac{2}{(\gamma+1)^2}\left(1+\frac{2-\gamma}{4}p_{0t}+\frac{\gamma-1}{16\gamma}p_{0t}\right)\frac{1}{M_\infty^2}, \quad (18c)$$

where p_{0t} is the limit of dimensionless Rayleigh pitot pressure as $M_\infty \to \infty$, which is a function of γ alone. In obtaining (18*c*), terms involving $(\gamma-1)^2/(\gamma+1)^2 M_\infty^2$, etc. are neglected. Some numerical examples of this formula can be found in table 1. They show satisfactory agreement with the results obtained by other methods.

Before we can work out the second iteration of the first-order quantities, we must obtain the first iteration of the second-order quantities, because v_1 and v_2 are of the same order of magnitude and we must take both quantities into account for the next iteration.

The equations to be used for determining the quantities u_2, v_2, p_3 and ρ_3 are (16), (2*b*), (3*c*), (4*c*), etc. First, eliminating ρ_3 from (3*c*) and (4*c*), we have

$$p_3 = -\rho_1\left(\frac{v_2^2}{2}+u_1u_2-v_1v_2+v_1v_3\right)-\frac{b}{(\gamma-1)c}p_1\psi_2+\frac{\gamma p_1\rho_2^2}{2\rho_1^2}-\frac{d}{(\gamma-1)c}p_1\psi_1^2. \quad (19)$$

Substituting (19) in (2*b*), we can obtain

$$u_2'+\frac{u_2}{r} = -\frac{2b\gamma}{(\gamma-1)c}p_1 r\frac{\rho_2}{\rho_1}-\frac{4d}{(\gamma-1)c}p_1\rho_1 v_1 r^3+\frac{1}{r}(3v_2-4v_3). \quad (20)$$

In this expression the last terms within the parentheses can be neglected for the first iteration, since they are of smaller magnitude than the other terms. By the same arguments which allowed the quantities p_1 and ρ_1 to be written as p_0 and ρ_0, v_1 can be expressed as in (18), and ρ_2 is obtained from (3*b*) and (4*b*) by eliminating p_2. After neglecting the small terms a simplified form is then

$$\rho_2 = -\frac{\rho_0^2}{\gamma p_0}\frac{u_1^2}{2}-\frac{b}{(\gamma-1)c}\rho_0^2 v_1 r^2. \quad (20a)$$

After simplification, (20) is now integrable and the result is

$$u_2 = \frac{H_1}{r}+H_2-H_3r^3+H_4r^4+H_6r^6, \quad (21)$$

where H_1 is an integration constant, and $H_2 \ldots H_6$ have the following form:

$$H_2 = \frac{1}{4}\frac{b}{(\gamma-1)c}\rho_0 G^2,$$

$$H_3 = \frac{1+3\gamma}{24}\frac{b}{(\gamma-1)c}\rho_0 AG-\frac{d}{(\gamma-1)c}p_0\rho_0 G,$$

$$H_4 = \frac{\gamma}{10}\frac{b}{(\gamma-1)c}\rho_0 AE-\frac{4}{5}\frac{d}{(\gamma-1)c}p_0\rho_0 E,$$

$$H_6 = \frac{1-3\gamma}{252}\frac{b}{(\gamma-1)c}\rho_0 A^2+\frac{2}{21}\frac{d}{(\gamma-1)c}p_0\rho_0 A.$$

Using (1*b*), after some manipulations, we find the solution of v_2 to be

$$v_2 = \frac{J}{r^2} + L_{-2}\left(\frac{G}{r^3} + \frac{E}{r^2}\right) + 4H\frac{1}{r} + L_0 + L_1 r + L_2 r^2 + L_3 r^3 + L_4 r^4 + L_6 r^6, \quad (22)$$

where J is an integration constant and the coefficients L_i are

$$L_{-2} = \frac{1}{8}\frac{\rho_0}{\gamma p_0}G^2, \quad L_0 = \frac{3+10\gamma}{4\gamma}\frac{b}{(\gamma-1)c}\rho_0 G^2,$$

$$L_1 = -\frac{1+8\gamma}{3\gamma}\frac{b}{(\gamma-1)c}\rho_0 GE, \quad L_2 = \frac{b}{(\gamma-1)c}\rho_0 E^2,$$

$$L_3 = \left(\frac{7-3\gamma}{30} - \frac{1}{15\gamma}\right)\frac{b}{(\gamma-1)c}\rho_0 AG + \frac{4}{5}\frac{d}{(\gamma-1)c}p_0\rho_0 G,$$

$$L_4 = \left(\frac{3\gamma-10}{45} + \frac{1}{18\gamma}\right)\frac{b}{(\gamma-1)c}\rho_0 AE - \frac{8}{15}\frac{d}{(\gamma-1)c}p_0\rho_0 E,$$

$$L_6 = \left(\frac{8-3\gamma}{504} - \frac{1}{216\gamma}\right)\frac{b}{(\gamma-1)c}\rho_0 A^2 + \frac{1}{21}\frac{d}{(\gamma-1)c}p_0\rho_0 A.$$

Now we are ready to calculate the second iteration of the first-order quantities. First, we express p_1 in the form of the second iteration by taking one more term in (15),

$$\underline{p_1} = p_0 - \tfrac{1}{2}\rho_0 v_1^2,$$

or

$$\underline{p_1} = p_0 - \tfrac{1}{2}\rho_0(E - Gr^{-1} - \tfrac{1}{6}Ar^2)^2, \quad (23)$$

where the bar underlining a symbol refers to the second interation quantity. Next we substitute (18), (22) and (23) into (14). After integration, we find that u_1 of the second iteration is

$$\underline{u_1} = L_{-2}Gr^{-3} + 2Jr^{-2} + 2EL_{-2}r^{-2} - (8H_1 + G)r^{-1}\log r + S_0 + S_1 r + S_2 r^2 + S_3 r^3 + S_4 r^4 + S_6 r^6 + Sr^{-1}, \quad (24)$$

where S is an integration constant, and the coefficients $S_0, S_1 \ldots$ are

$$S_0 = E - \frac{3+8\gamma}{2\gamma}\frac{b}{(\gamma-1)c}\rho_0 G^2, \qquad S_1 = \frac{5\gamma+1}{3\gamma}\frac{b}{(\gamma-1)c}\rho_0 GE,$$

$$S_2 = -\frac{A}{18} - \frac{1}{3}\frac{b}{(\gamma-1)c}(2p_0 + \rho_0 E^2), \quad S_3 = \frac{1}{12}\frac{b}{(\gamma-1)c}\rho_0 AG - \frac{L_3}{2},$$

$$S_4 = -\frac{1}{15}\frac{b}{(\gamma-1)c}\rho_0 AE - \tfrac{2}{5}L_4, \qquad S_6 = \frac{1}{252}\frac{b}{(\gamma-1)c}\rho_0 A^2 - \tfrac{2}{7}L_6.$$

Similarly, from (17), by writing u_1 as

$$u_1 = v_1 + \tfrac{1}{2}r[1 - (\rho_0 v_1^2/\gamma p_0)]v_1'$$

we can find the solution of v_1 for the second iteration to be

$$\underline{v_1} = I + I_{-3}r^{-3} + I_{-2}r^{-2} + I_{-1}r^{-1} + I'_{-1}r^{-1}\log r + I'_1 \log r + I_1 r + I_2 r^2 + I_3 r^3 + I_4 r^4 + I_6 r^6 - 2Sr^{-1} + \tfrac{1}{3}\rho_0(E - Gr^{-1} - \tfrac{1}{6}Ar^2)^3/\gamma p_0, \quad (25)$$

where I is an integration constant, and the coefficients I_i are

$$I_{-3} = -\tfrac{2}{3}GL_{-2}, \qquad I_{-2} = -2(J+EL_{-2}), \qquad I_{-1} = 16H_1,$$
$$I'_{-1} = 2(8H_1+G), \qquad I'_1 = 2(S_0-E), \qquad I_1 = 2S_1$$
$$I_2 = S_2+\tfrac{1}{6}A, \qquad I_3 = \tfrac{2}{3}S_3, \qquad I_4 = \tfrac{1}{2}S_4, \quad I_6 = \tfrac{1}{3}S_6.$$

Thus far we can describe the flow field in the shock layer of the complete second-order approximation in terms of elementary functions. In summary we can write

$$\left.\begin{aligned} u(r,\theta) &= \underline{u_1}\sin\theta + u_2\sin^3\theta + \ldots, \\ v(r,\theta) &= -\underline{v_1}\cos\theta - v_2\sin^2\theta\cos\theta - \ldots, \\ p(r,\theta) &= \cos^2\theta(\underline{\pi_1} + \pi_2\sin^2\theta + \pi_3\sin^4\theta + \ldots). \end{aligned}\right\} \tag{26}$$

The coefficients $\underline{u_1}\ldots v_2$ in the first two equations are the solutions obtained above, and the coefficients in the pressure equation are

$$\underline{\pi_1} = \underline{p_1} \quad \text{as in (23)},$$
$$\pi_2 = p_0 - \tfrac{1}{2}\rho_0 u_1^2 - \tfrac{1}{4}A\rho_0 v_1 r^2,$$
$$\pi_3 = \pi_2 - \rho_0 u_1 u_2 - \tfrac{1}{8}Ar^2(\rho_0 v_2 + \rho_2 v_1) + \frac{\gamma p_0 \rho_2^2}{2\rho_0^2} - \frac{d}{(\gamma-1)c}p_0\rho_0^2 v_1^2 r^4.$$

The expressions for u_1, v_1, u_2 and v_2 are found in (16), (18), (21) and (22) respectively, and the expression for ρ_2 is indicated in (20a). The pressure equation has one term more than the first two equations. This should not be regarded as inconsistency; rather it is a term acquired in the process of calculation and is included to achieve better accuracy. This will be called the 'pseudo' third-order approximation.

In order to determine the second iteration of the second-order quantities, we must obtain the solutions for the first iteration of the third-order quantities. In fact this principle of alternate calculations (i.e. higher iterations for lower-order quantities are necessarily preceded by lower iterations for higher-order quantities) applies to all iterations. Thus, we can, in principle, carry out the improvement indefinitely in a consistent manner for higher orders and higher iterations, if necessary. However, the labour involved in the algebraic manipulation increases rapidly for the higher iterations. Moreover, it may not be essential to acquire the higher iterations, since the agreement with 'exact' numerical results is already good, as will be shown below. We shall, therefore, calculate a few examples in the next section using the existing solutions of (26) and make comparisons with numerical results, before the third-order approximation is given.

5. Calculations

The equations for determining the various integration constants are given above. The boundary conditions for determination of these integration constants are the properly expanded Rankine–Hugoniot relations at the shock wave. Unless the shock shape is specified beforehand, the integration constants cannot be evaluated explicitly but rather are functions of the shock configuration parameters and the standoff distance. In order to determine these functions of the

integration constants, we must at the same time consider the boundary conditions on the body surface. The end result is then a system of non-linear simultaneous algebraic equations and after solving these equations, a pair of roots corresponding to the standoff distance and the shock angles can be selected. Once the shock wave shape is known, the integration constants can be easily computed, thus the flow field in the shock layer is determined. The co-ordinate system for such a direct problem should be chosen in such a way that the body

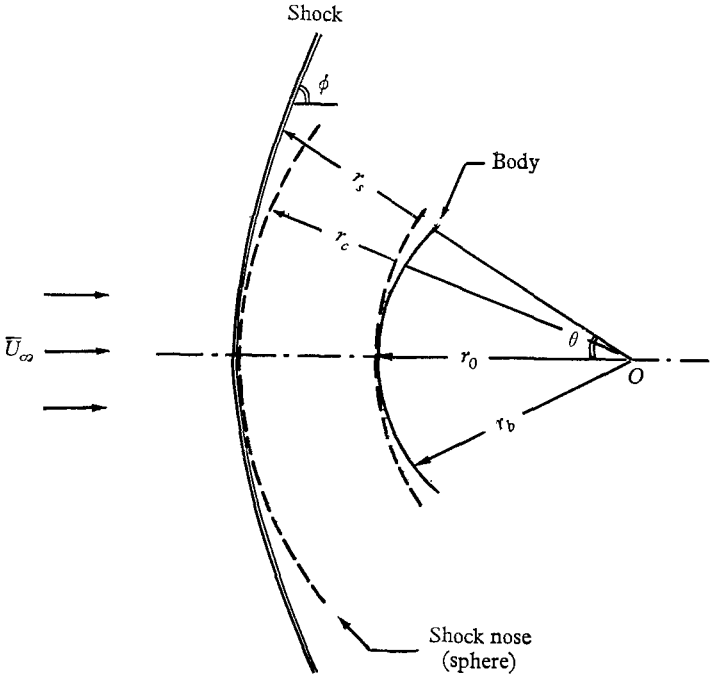

FIGURE 2. Shock wave and body configuration.

surface can be simply described. While it appears that we have formulated a truly direct method for a blunt body problem, it should be noted that in order to find the roots of a system of non-linear simultaneous equations of high degrees, an iteration procedure such as Newton's method must be employed. The process is inevitably very laborious. However, if we do not take such a direct course but look at it as an inverse problem where the shock shape is prescribed beforehand for each computation, the complexity is greatly reduced, since in this way only a simple algebraic equation is to be solved.

For the above reasons, the examples given below are all inverse problems. The origin of the co-ordinate system is chosen to lie at the centre of curvature of the shock wave (figure 2), and the shock wave is expressed in a power series form as

$$r_s = r_c + \alpha \sin^2\theta + \beta \sin^4\theta + \xi \sin^6\theta + \ldots, \tag{27}$$

where α, β and ξ are the configuration coefficients and r_c is actually unity. In order to be able to carry out a one-parameter iteration and to facilitate compari-

son against Van Dyke & Gordon's (1959) results, the shape of the shock wave is assumed to be a conic section. The equation of this conic section is written as

$$y^2 = 2r_c x - B_c x^2 \tag{28}$$

in a rectangular co-ordinate system whose origin lies on the shock at the symmetric point. It is then possible to relate B_c to the shock configuration coefficients in (27) by geometric considerations. The final form is

$$r_s = r_c + \tfrac{1}{8} r_c (1 - B_c) \sin^4\theta + \tfrac{1}{16} r_c B_c (1 - B_c) \sin^6\theta - \ldots. \tag{29}$$

Notice that the coefficient for $\sin^2\theta$ term is missing; this is due to the fact that the origin of the co-ordinate system coincides with the centre of the shock curvature.

In order to expand the Rankine–Hugoniot relations, we must associate the shock angle ϕ with θ (see figure 2). By geometric considerations, the relation is

$$\sin^2\phi = 1 - \sin^2\theta + 8\frac{\beta}{r_c}\sin^4\theta + \left(12\frac{\xi}{r_c} - 8\frac{\beta}{r_c} - 16\frac{\beta^2}{r_c^2}\right)\sin^6\theta + \ldots. \tag{30}$$

Substituting this relationship in (7)–(10), we have

$$\left.\begin{aligned} u_{1s} &= 1, & v_{1s} &= \frac{\gamma-1}{\gamma+1} + \frac{2}{(\gamma+1)M_\infty^2}, \\ p_{1s} &= \frac{2}{\gamma+1} - \frac{\gamma-1}{\gamma(\gamma+1)M_\infty^2}, & \rho_{1s} &= \frac{1}{v_{1s}}, \end{aligned}\right\} \tag{31}$$

$$\left.\begin{aligned} u_{2s} &= -\frac{8}{\gamma+1}\left(1 - \frac{1}{M_\infty^2}\right)\frac{\beta}{r_c}, & v_{2s} &= \frac{2}{\gamma+1}\frac{1}{M_\infty^2}, \\ p_{2s} &= -\frac{2}{\gamma+1}, & \rho_{2s} &= \frac{-2(\gamma+1)M_\infty^2}{[2+(\gamma-1)M_\infty^2]^2}, \quad p_{3s} = \frac{16}{\gamma+1}\frac{\beta}{r_c}, \end{aligned}\right\} \tag{32}$$

where the subscripts 1 and 2 refer to the order of approximations. They have the same meaning as those used in (11*a*)–(11*d*). The third-order expressions can again be found in the appendix.

The tangency condition on the body surface is that the velocity component perpendicular to the surface equals zero. Since the co-ordinate system used here was chosen to permit convenient specifications of the shock wave shape, its origin coincides with the radius centre of the shock-nose curvature. However, the radius centre of the body-nose curvature is, in general, not at the origin of the co-ordinate system. We must, therefore, expand the velocity components in order to find the normal component at the surface. We first assume that the body section, which is not necessarily a conic section, can be written as

$$r_b = r_0 + \mu\sin^2\theta + \nu\sin^4\theta + \ldots, \tag{33}$$

and then we relate the coefficients $\mu, \nu, \ldots$ to the velocity components, so that these coefficients can be evaluated after the shock shape is specified. Here the subscript b refers to the quantity at the body surface and the subscript 0 refers

to the quantity at the stagnation point. Note that the coefficient of $\sin^2\theta$ is not necessarily zero. The individual velocity components at $r = r_b$ can be expanded as

$$\left.\begin{aligned} v_1(r_b) &= v_1(r_0) + (r_b - r_0)v_1'(r_0) + \frac{(r_b-r_0)^2}{2!}v_1''(r_0) + \frac{(r_b-r_0)^3}{3!}v_1'''(r_0) + \ldots, \\ v_2(r_b) &= v_2(r_0) + (r_b - r_0)v_2'(r_0) + \frac{(r_b-r_0)^2}{2!}v_2''(r_0) + \ldots, \\ v_3(r_b) &= v_3(r_0) + (r_b - r_0)v_3'(r_0) + \ldots, \\ u_1(r_b) &= u_1(r_0) + (r_b - r_0)u_1'(r_0) + \ldots, \\ &\ldots\ldots\ldots\ldots\ldots\ldots\ldots\ldots\ldots\ldots\ldots\ldots\ldots\ldots\ldots\ldots\ldots\ldots\ldots\ldots\ldots\ldots \end{aligned}\right\} \tag{34}$$

No symbol is given here to indicate the degree of iterations; the form of these expansions is the same for any iteration. Thus, v_1 can be actually v_1 or $\underline{v_1}$. Substituting these expansions in (11) and using geometrical considerations, we find the normal velocity component on the body to be

$$q_\perp = -v_1(r_0)\cos\theta - \left[\frac{2\mu}{r_0}u_1(r_0) - 2\left(\frac{\mu}{r_0}\right)^2 v_1(r_0) + \mu v_1'(r_0) + v_2(r_0)\right]\sin^2\theta\cos\theta - \ldots. \tag{35}$$

The third-order term in this equation can be found in the appendix.

The tangency condition for an arbitrary body surface is that each coefficient of $q_\perp$ equals zero individually. Thus, we have

$$v_1(r_0) = 0. \tag{35a}$$

This condition determines the radial distance of the stagnation point, i.e. the standoff distance, for any order of approximation.

The second coefficient in (35) determines the second-order body configuration coefficient, which is

$$\mu = \frac{-v_2(r_0)}{2(u_1(r_0)/r_0) + v_1'(r_0)}. \tag{35b}$$

We shall now discuss briefly how to apply the shock relations as boundary conditions to evaluate the integration constants. Because quantities in (31) and (32) are given at $r = r_s$, they must be transferred to the values at $r = r_c = 1$ for evaluation of the integration constants. The form of the expansion is very similar to those indicated in (34). Using the pressure as an example, we have

$$p_s = p_1(r_c) + p_2(r_c)\sin^2\theta + [p_3(r_c) + (\beta/r_c)p_1'(r_c)]\sin^4\theta + \ldots,$$

but by definition at the shock wave

$$p_s = p_{1s} + p_{2s}\sin^2\theta + p_{3s}\sin^4\theta + \ldots,$$

hence, we have

$$\left.\begin{aligned} p_1(1) &= p_{1s}, \\ p_2(1) &= p_{2s}, \\ p_3(1) &= p_{3s} - \beta p_1'(1). \end{aligned}\right\} \tag{36}$$

Similar expressions can be obtained from the other flow quantities. Using the expanded Rankine–Hugoniot relations in (31) and (32) transferred to $r_c = 1$, the integration constants G, E, H_1, J, S and I in (16) to (25), and the coefficients c,

b and d in (4a), (4b) and (4c) can now be evaluated. They, however, contain the parameters M_∞, γ and β. A few examples of these constants are

$$G = 2+\frac{A}{3},$$

$$E = \frac{\gamma-1}{\gamma+1}+\frac{2}{(\gamma+1)M_\infty^2}+G+\frac{A}{6},$$

$$H_1 = -\frac{8}{\gamma+1}\left(1-\frac{1}{M_\infty^2}\right)\beta - H_2+H_3-H_4-H_6.$$

After all the integration constants are obtained, we can then use the tangency condition $v_1 = 0$ to find the roots of (25). One of the roots $r = r_0$ is the distance of the stagnation point on the axis of symmetry; the others are ruled out on the physical grounds. Since this is a ninth degree equation, the roots are found by applying Newton's method. Once r_0 is known, the coefficient μ can be calculated easily. Thus, the flow field and the body surface in the shock layer are determined. Notice that for a given value of r_0 the coefficient μ only determines the body-nose radius precisely. For bodies such as spheres, the two-term approximation of (33) is a good approximation. But for bodies of more general shapes, a three-term approximation may be required. There are certainly limitations in describing body shapes by such series expansion techniques, since the series expansion is inefficient for very blunt shapes, and may even fail in other cases.

A number of examples have been computed for various free-stream Mach numbers and the shock configuration constants β. The ratio of the specific heats was chosen to be 1·4 for all the examples. Both the 'true' second-order and the 'pseudo' third-order approximations have been calculated, but differences are not significant. The results of the pseudo third-order approximation are shown in figures 3–6, together with numerical results by the marching technique and the experimental measurements (Kendall 1959; Xerikos & Anderson 1965).

Since the shock wave is described by a two-term series, the coefficient β can be varied to affect the shape of the body surface. The effect of β on the body shape near the stagnation streamline is in general very small, but becomes noticeable near the sonic line. For instance, in calculating a spherical body the variation of β affects the body radius. Thus, a trial-and-error procedure must be employed to obtain the prescribed bodies.

Neglecting the terms of small magnitude to simplify momentum equations such as (14) is actually equivalent to neglecting them in entropy equations such as (13) and (19). We should use the approximate entropy equations consistent with the number of iterations. In order to evaluate the constant coefficients b, d, or e behind the shock wave, the entropy equations must, however, be used. Since the entropy equations are in approximate form, it seems reasonable to evaluate them approximately. On the other hand, since these coefficients contain the free-stream conditions as parameters, they should be independent of the approximation used. The latter argument is generally favoured here, and for lack of proper terminology this will be called the conventional procedure. It was found, however, that the approximate evaluation of the coefficients gives slightly better

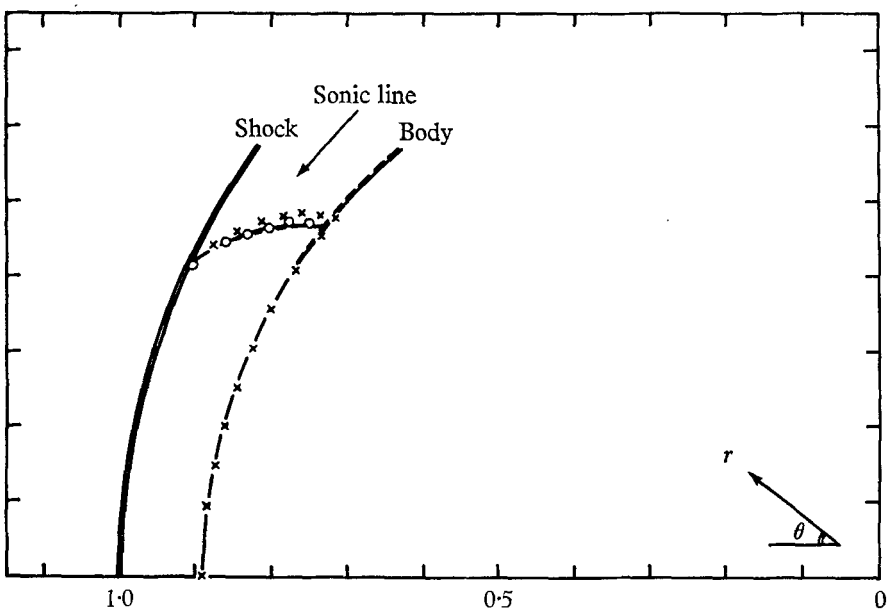

FIGURE 3. Spherical body and sonic line configuration at $M_\infty = 6{\cdot}0$, $\gamma = 1{\cdot}4$. – – –, pseudo third-order (constants conventional); ○, third order (constants approximate); ——, third order (constants conventional); ×, Van Dyke & Gordon.

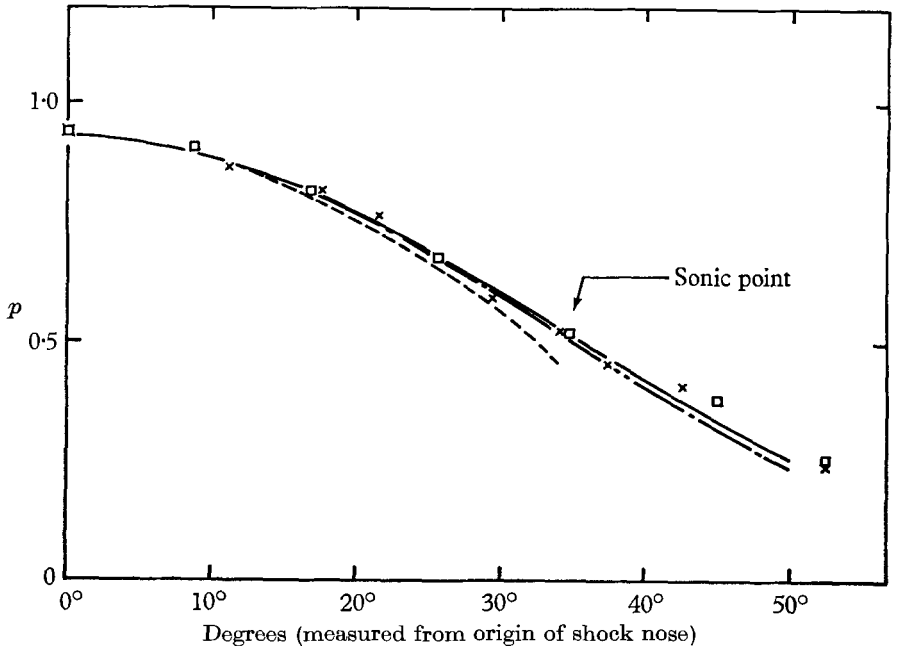

FIGURE 4. Surface pressure distribution at $M_\infty = 6{\cdot}0$, $\gamma = 1{\cdot}4$. Theoretical: ——, third order (constants approximate); – – –, third order (constant conventional); – – –, Van Dyke & Gordon. Experimental: ×, Kendall ($M_\infty = 4{\cdot}76$); □, Xerikos & Anderson ($M_\infty = 4{\cdot}93$).

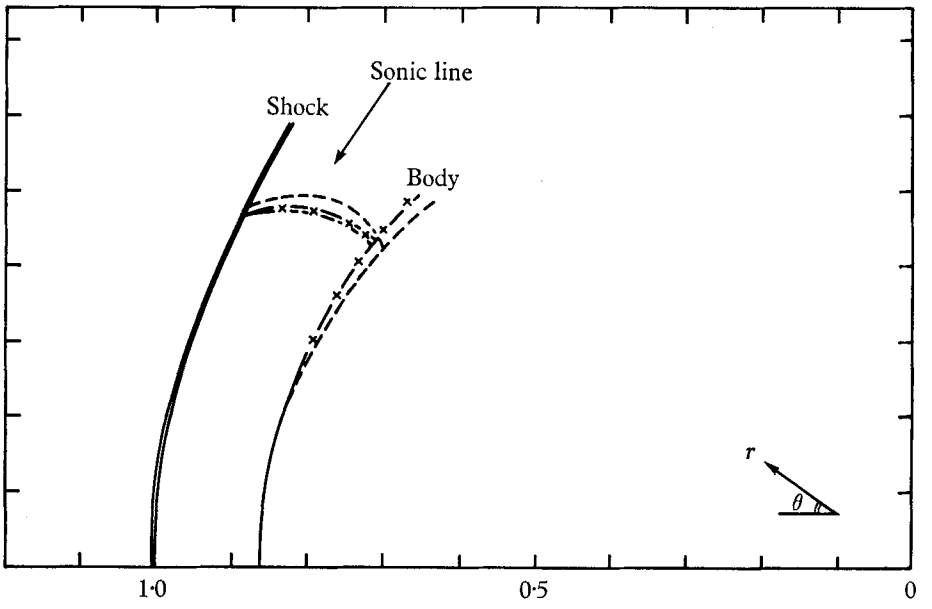

FIGURE 5. Spherical body and sonic line configuration at $M_\infty = 3{\cdot}0$, $\gamma = 1{\cdot}4$. ×, pseudo third order (constants conventional); ——, third order (constants approximate); ——, third order (constants conventional); – – –, Van Dyke & Gordon.

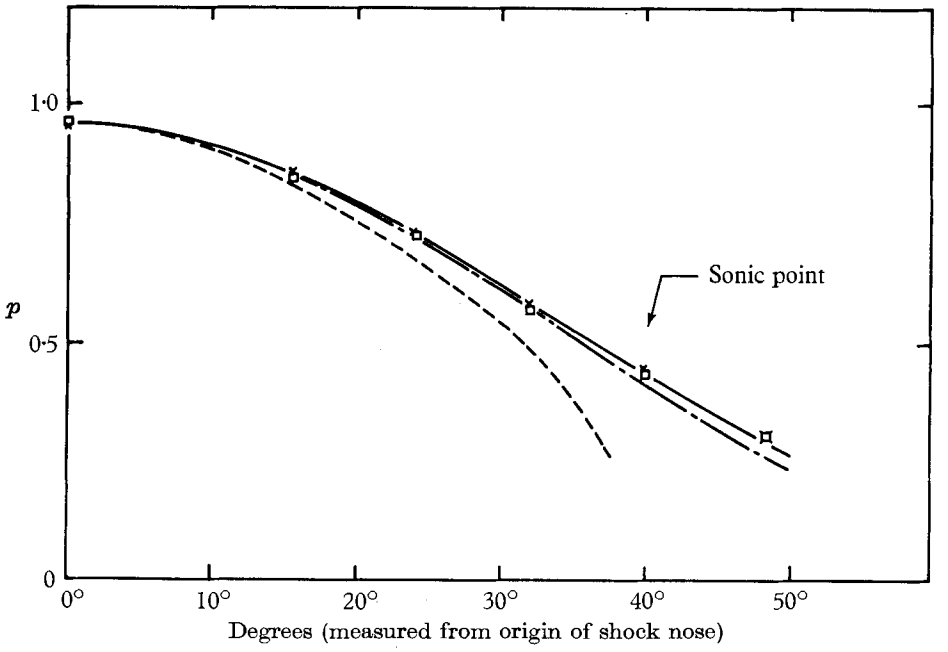

FIGURE 6. Surface pressure distribution at $M_\infty = 3{\cdot}0$, $\gamma = 1{\cdot}4$. Theoretical: ——, third order (constants approximate); ——, third order (constants conventional); – – –, Van Dyke & Gordon. Experimental: ×, Kendall ($M_\infty = 2{\cdot}81$); □, Xerikos & Anderson ($M_\infty = 3{\cdot}0$).

results. Both approaches were taken for computing the examples. The results are shown in figures 3 to 6.

To recapitulate, the procedure for computing the flow field of a blunt body in a uniform free stream is as follows.

(*a*) Assume the shape of an initial shock wave.

(*b*) Relate the shock angle ϕ to the polar angle θ, and evaluate (31) and (32).

(*c*) Determine the constants c, b, d and the integration constants, which in turn, determine all other coefficients.

(*d*) Let $v_1 = 0$ in (25) and find the roots of this equation.

(*e*) Determine the coefficient μ. If the value of this coefficient is not within acceptable limits of the prescribed value, we must assume a new β and repeat steps (*a*)–(*e*) until the requirement is met.

For the direct problem, the procedure is essentially the same, except that the body co-ordinates should be adopted, and β is a parameter rather than an assumed number. Consequently, we have to solve a pair of simultaneous equations, (25) and (35*b*). One pair of roots is the required β and r_0. Once β and r_0 are known, the rest of the calculation is straightforward.

The standoff distances for second iteration are given in table 2, along with those given by the first iteration. The constants in the entropy equations were determined by the conventional procedure.

		Standoff distance		
M_∞	γ	First iteration	Second iteration	Van Dyke & Gordon (1959)
3	1·4	0·133	0·1366	0·1351
6	1·4	0·106	0·1091	0·1085
10^4	1·4	0·0960	0·0990	0·0983

TABLE 2. Standoff distances of spheres

Figures 3 and 4 show the flow fields for spherical bodies calculated by the above formulas for $M_\infty = 6{\cdot}0$ and $\gamma = 1{\cdot}4$. The bluntness coefficient B_c was chosen to be 0·47, which is the same as that given by Van Dyke & Gordon (1959). There are essentially two sets of curves plotted in these diagrams in addition to those of the third-order approximations and those obtained by numerical integration. One set of curves is based on constants in the entropy equations which were determined by the conventional procedure, and the other on constant d which was determined approximately. (Even in the latter, the constant b was determined conventionally, since b appears in the second-order quantities and the iterated first-order quantities.) It turned out that at such high Mach number the differences in the body shape and the sonic line in the two cases are so small that they are not discernible in this plot. Hence, no curve of the pseudo third-order approximation, whose constant d is determined approximately, is plotted in figure 3. The gap between the dotted lines and the solid ones was actually somewhat enlarged, so that the diagram could be inked. There is, however, a difference in the pressure distributions on the surface of the two cases shown in figure 4. (The

curves in figure 4 are actually designated as the third order. However, they also refer to the pseudo third order, since to the order of approximation considered here they are the same.) Although the body in figure 3 appears to coincide with that by Van Dyke & Gordon, the radii of the spheres were found to be different, ours being 0·760 and theirs being 0·732. This perhaps indicates the somewhat arbitrary manner of fitting a sphere to the second-order body description.

Since the experimental data shown in figure 4 were taken at stations on the sphere, we had to convert their locations to the values of θ in the present coordinate system. The process of conversion involves the radius of the sphere. The one which we used was the radius of sphere obtained by the present calculation. If we were to use the radius obtained by Van Dyke & Gordon, the experimental surface pressure distribution in figure 4 will be slightly shifted.

The above example demonstrates the accuracy of the present method, at least for the flows past a sphere with relatively high Mach numbers. It is, however, still of value to consider an example at relatively low Mach number, say $M_\infty = 3{\cdot}0$, and to examine its accuracy as compared with numerical results and experimental measurements. The flow field and the body configurations of this example are shown in figures 5 and 6. Again the bluntness coefficient B_c was chosen to be the same as that given by Van Dyke & Gordon for this case; i.e. 0·25. Two ways to determine the constants in the entropy equations were considered. The results again indicate that the body configurations and the sonic lines for these two cases are almost identical to the scale we chose for the plot. Hence, only curves whose coefficients were determined conventionally are plotted. The body configurations obtained by Van Dyke & Gordon appear to recede more than those computed by present method. This probably constitutes the reason that the surface pressure distribution in Van Dyke's computation is much lower than ours (figure 6). The discrepancy is actually quite large near the sonic point.

As a last example, we consider the test case given by Van Dyke (1965) of a paraboloidal shock wave with $M_\infty \to \infty$ and $\gamma = 1{\cdot}4$. Unfortunately, the results obtained by the present method did not agree well with the results by the other methods. If we make the surface pressure distributions identical in the two cases, a discrepancy shows up in the body configuration, where there is approximately 15 % difference in radius. It was thought that this was due to the inaccuracy of the pseudo third-order approximation, since it uses a two-term description of the body shape, which determines only the body nose radius. For the paraboloid body this description may not be adequate. Consequently, the third-order approximation was calculated, but the improvement was rather insignificant. The same type of difficulty was encountered by Swigart (1963).

Swigart later suggested that if we replace $\sin\theta$ by $\sin\theta/(1+\sin^2\theta)^{\frac{1}{2}}$ and $\cos\theta$ by $[1-\sin^2\theta/(1+\sin^2\theta)]^{\frac{1}{2}}$ in the expansion scheme of (11), the results may be improved. Following this suggestion it turns out that the final form of the second-order solutions remain unaltered, though (26), (3c) and (4c) appear in the different forms provided that certain steps are taken in the algebraic manipulation. Computations were subsequently made, but the improvement was still unsatisfactory. The results are, nevertheless, tabulated in table 3 against those obtained by Lomax & Inouye which are considered accurate to four figures. The

values given by Lomax & Inouye in table 3 are their unpublished results based on their refined procedure (1964), taken from Van Dyke's (1965) paper.

In this table, M refers to the surface Mach number. In the computation of the present table, the coefficient d was evaluated approximately. If it were determined by the conventional procedure, the results would change slightly. We may conjecture that the discrepancy in the body shape is still due to the inadequacy of the pseudo third-order approximation. However, no third-order approximations have been carried out yet, since the solutions given in the appendix can no longer be used without substantial changes.

NASA results				Present results				
p	x	y	M	p	x	y	M	θ
0·9199	0·0989	0	0	0·9199	0·0987	0	0	0
0·8926	0·1089	0·12	0·208	0·8926	0·109	0·125	0·216	7° 57′
0·8179	0·1389	0·24	0·413	0·8179	0·139	0·245	0·434	15° 54′
0·7129	0·1896	0·36	0·614	0·7129	0·187	0·359	0·650	23° 49′
0·5974	0·2621	0·48	0·810	0·5974	0·250	0·465	0·860	31° 48′
0·4868	0·3576	0·60	0·998	0·4868	0·329	0·563	1·06	40° 0′

TABLE 3. Surface values for the test example (paraboloidal shock, $M_\infty = 10^4$, $\gamma = 1{\cdot}4$)

6. Third-order approximation

The differential equations, the boundary conditions, and the solutions are shown in the appendix. The solutions are obtained in a similar manner as shown above for the second-order solutions. They are in the form of the first iteration. The availability of these makes it possible to calculate the second iteration of the second-order solutions which can, in turn, be used to calculate the third iteration of the first-order solutions. Thus, it completes the third cycle of improvement. However, no actual work has been carried out here, since the manipulation is rather lengthy.

Although the complete third-order approximation has not been worked out, third-order approximations were calculated; namely, u_3 and v_3 terms are added in (26). The results of the third-order approximation for $M_\infty = 3{\cdot}0$ and $M_\infty = 6{\cdot}0$ can be seen in figures 3–6. Both cases in which the coefficients were determined approximately and conventionally were considered. However, only curves of one case are plotted, unless the differences are large enough to warrant designation of two separate curves for two different cases in the plot. The pseudo third-order approximations (actually the second order) shown in figures 3–6 are all very close to the third-order approximations. This at least demonstrates the self consistency of the scheme, especially when a mathematical proof of the series convergence is not feasible.

7. Discussion

In the above we have used the expansion scheme to determine the flow field in the subsonic region. A natural question is the interdependence of the elliptical equations. In the present case, since the expansion proceeds outward from the

stagnation region to the supersonic region, a given point is influenced by the conditions at other points downstream. In other words, the calculation of the first-order quantities is affected by the higher-order quantities which are subject to the boundary conditions away from the stagnation point. For instance, (14) contains the quantity v_2. Similar situations exist in all higher-order equations. However, the coupling has been shown to be rather weak. For this reason we must perform the alternate calculations, since we are not able to work out higher iterations for any low-order solutions without taking into account the backward influence. The present approach is probably not an efficient method to treat a body with sonic corners, since the presence of a sonic corner generates large backward influence which is felt throughout the entire subsonic region.

It is not clear, at present, what the appropriate expansion scheme should be for a particular type of body. As we have demonstrated, the scheme used above is particularly good for predicting the flow field over a sphere. Even if other expansion schemes are adopted, the procedures of the present analysis will remain valid.

We have only considered the symmetrical cases in this study. However, extension of the present formulation to the blunt body in a supersonic stream at a small angle of attack seems feasible. It may be perturbed about the flow at zero incidence as was carried out by Swigart (1963).

The writer is indebted to S. A. Powers of Northrop Norair for his critical reading of the manuscript and to the referee for pointing out an algebraic error in the Northrop report (NOR 65-239, September, 1965) on which this paper is based.

Appendix

In this appendix, equations, boundary conditions, and solutions of the third-order approximations are given without explanation. They are, however, labelled in such a way that we can easily associate them with the second-order counterparts.

Governing equations:

$$r(\rho_1 v_3+\rho_2 v_2+\rho_3 v_1)'+2(\rho_1 v_3+\rho_2 v_2+\rho_3 v_1)-6(\rho_1 u_3+\rho_2 u_2+\rho_3 u_1)=0, \quad (1c)$$

$$6\frac{p_4}{r}+\rho_1\left(-v_1u_3'-v_2u_2'-v_3u_1'+\frac{6u_1u_3+3u_2^2}{r}-\frac{u_1v_3+u_2v_2+u_3v_1}{r}\right)$$

$$+\rho_2\left(-v_1u_2'-v_2u_1'+\frac{4u_1u_2}{r}-\frac{u_1v_2+u_2v_1}{r}\right)+\rho_3\left(-v_1u_1'+\frac{u_1^2-u_1v_1}{r}\right)=0, \quad (2c)$$

$$\frac{p_4}{\rho_1}-p_3\frac{\rho_2}{\rho_1^2}+\frac{p_2}{\rho_1^2}\left(\frac{\rho_2^2}{\rho_1}-\rho_3\right)+\frac{p_1}{\rho_1^2}\left(\frac{2\rho_2\rho_3}{\rho_1}-\frac{\rho_2^3}{\rho_1^2}-\rho_4\right)$$

$$+k(u_2^2-v_2^2+2u_1u_3-2v_1v_3+2v_2v_3+2v_1v_4)=0, \quad (3d)$$

$$p_4=\rho_1^\gamma(b\psi_3+2d\psi_1\psi_2+e\psi_1^3)+\rho_1^{\gamma-1}(c\gamma\rho_4+b\gamma\rho_3\psi_1$$

$$+d\gamma\rho_2\psi_1^2+b\gamma\rho_2\psi_2)+\gamma(\gamma-1)\rho_1^{\gamma-2}[\tfrac{1}{2}b\rho_2^2\psi_1+c\rho_2\rho_3]$$

$$+\tfrac{1}{6}[\gamma(\gamma-1)(\gamma-2)]c\rho_1^{\gamma-3}\rho_2^3=0. \quad (4d)$$

Boundary conditions:

$$\left.\begin{aligned}
u_{3s} &= \frac{8}{\gamma+1}\frac{\beta}{r_c} - \frac{12}{\gamma+1}\left(1-\frac{1}{M_\infty^2}\right)\frac{\xi}{r_c},\\
v_{3s} &= \frac{1}{\gamma+1}\left(1+\frac{1}{M_\infty^2}\right) - \frac{1}{\gamma+1}\left(1-\frac{1}{M_\infty^2}\right)\left(1-8\frac{\beta}{r_c}\right) - \frac{16}{\gamma+1}\frac{\beta}{r_c},\\
p_{3s} &= \frac{16}{\gamma+1}\frac{\beta}{r_c},\\
\rho_{3s} &= -\rho_{2s}\left[8\frac{\beta}{r_c} - \frac{(\gamma-1)M_\infty^2}{2+(\gamma-1)M_\infty^2}\right],\\
p_{4s} &= \frac{8}{\gamma+1}\left(3\frac{\xi}{r_c} - 2\frac{\beta}{r_c} - 4\frac{\beta^2}{r_c^2}\right),
\end{aligned}\right\} \tag{32a}$$

$$\nu = -\frac{v_3(r_0)+\mu\left[\dfrac{2u_2(r_0)}{r_0}+v_2'(r_0)\right]+\mu^2\left[\dfrac{2u_1'(r_0)}{r_0}-\dfrac{2u_1(r_0)}{r_0^2}+\dfrac{v_1''(r_0)}{2}\right]}{4\dfrac{u_1(r_0)}{r_0}+v_1'(r_0)}. \tag{35c}$$

Differential equation for the tangential velocity component can be reduced to:

$$u_3'+\frac{u_3}{r} = -b\gamma\rho_1^{\gamma-2}\rho_2^2 r - \frac{2b\gamma}{\gamma-1}\rho_1^{\gamma-1}\rho_3 r - \frac{2d}{\gamma-1}\rho_1^{\gamma}(\rho_1 v_2+\rho_2 v_1)r^3$$
$$-\frac{6e}{\gamma-1}\rho_1^{\gamma+2}v_1^2 r^5 - \frac{4\gamma d}{\gamma-1}\rho_1^{\gamma}\rho_2 v_1 r^3 + \frac{1}{r}(5v_3-6v_4).$$

This equation can be solved approximately as

$$u_3 = \frac{\bar{Q}}{r}+\frac{Q_{-2}}{r^2}+Q_0+Q_1 r+Q_2 r^2+Q_3 r^3+Q_4 r^4+Q_5 r^5+Q_6 r^6+Q_7 r^7+Q_8 r^8+Q_{10} r^{10}, \tag{21a}$$

where $\bar{Q}$ is an integration constant. The coefficients $Q_{-2}\ldots Q_{10}$ are

$$\begin{aligned}
Q_{-2} &= -\tfrac{1}{16}N_1 G^4,\\
Q_0 &= \tfrac{1}{2}N_4 G H_1,\\
Q_1 &= \tfrac{1}{8}(-\tfrac{1}{3}N_1 A G^3 + 2N_4 G H_2 + (\rho_0^2 N_5 G^3/\gamma p_0) - N_2 G^3),\\
Q_2 &= \tfrac{1}{3}(\rho_0 N_5 J + \tfrac{1}{4}N_2 G^2 E),\\
Q_3 &= \rho_0 N_5 H_1 - \tfrac{1}{24}N_4 A H_1,\\
Q_4 &= \tfrac{1}{5}(\tfrac{1}{24}N_1 A^2 G^2 + N_3 G^2 - \tfrac{1}{2}N_4 G H_3 - \tfrac{1}{6}N_4 A H_2 + \tfrac{1}{2}N_5 J_2 - \tfrac{1}{8}N_2 A G^2),\\
Q_5 &= \tfrac{1}{6}(-\tfrac{1}{6}N_2 A G E - 2N_3 G E + \tfrac{1}{2}N_4 G H_4 - \tfrac{2}{3}b\rho_0^2 N_5 G E/(\gamma-1)c),\\
Q_6 &= \tfrac{1}{7}N_3 E^2,\\
Q_7 &= \tfrac{1}{8}(-\tfrac{1}{108}N_1 A^3 G + \tfrac{1}{3}N_3 A G + \tfrac{1}{2}N_4 G H_5 + \tfrac{1}{6}N_4 A H_3 + \tfrac{1}{5}N_5 J_3),\\
Q_8 &= \tfrac{1}{9}(\tfrac{1}{36}N_2 A^2 E - \tfrac{1}{3}N_3 A E - \tfrac{1}{6}N_4 A H_4 + \tfrac{1}{6}N_5 J_4),\\
Q_{10} &= \frac{1}{11}\left(\frac{N_1 A^4}{6^4}+\frac{N_3 A^2}{36}-\frac{N_4 A H_5}{6}+\frac{N_5 J_5}{8}-\frac{N_2 A^3}{6^3}\right),
\end{aligned}$$

where
$$N_1 = -\frac{b}{4\gamma(\gamma-1)c}\frac{\rho_0^2}{p_0},$$
$$N_2 = -\left[\frac{b^2\gamma}{(\gamma-1)^2c^2}-\frac{2d}{(\gamma-1)c}\right]\rho_0^2,$$
$$N_3 = \left[-\frac{b^3\gamma}{(\gamma-1)^3c^3}(2\gamma-1)+\frac{6bd\gamma}{(\gamma-1)^2c^2}-\frac{6e}{(\gamma-1)c}\right]p_0\rho_0^2,$$
$$N_4 = \frac{2b}{(\gamma-1)c}\rho_0,$$
$$N_5 = \frac{b^2\gamma}{(\gamma-1)^2c^2}-\frac{2d}{(\gamma-1)c},$$
$$J_2 = \frac{3b}{(\gamma-1)c}\rho_0^2G^2+\frac{\rho_0^2}{\gamma p_0}\frac{AG^2}{4},$$
$$J_3 = -\frac{\gamma+1}{2}\frac{b}{(\gamma-1)c}\rho_0^2AG-\frac{1}{12}\frac{\rho_0^2}{\gamma p_0}A^2G+\frac{4d}{(\gamma-1)c}p_0\rho_0^2G,$$
$$J_4 = \frac{6\gamma+10}{15}\frac{b}{(\gamma-1)c}\rho_0^2AE-\frac{16}{5}\frac{d}{(\gamma-1)c}p_0\rho_0^2E,$$
$$J_5 = -\frac{2+\gamma}{21}\frac{b}{(\gamma-1)c}\rho_0^2A^2+\frac{1}{108}\frac{\rho_0^2}{\gamma p_0}A^3+\frac{8}{21}\frac{d}{(\gamma-1)c}p_0\rho_0^2A;$$

and
$$v_3 = -\frac{1}{\rho_0}(\rho_2v_2+\rho_3v_1)+\frac{\bar{\Omega}}{r^2}-\frac{\Omega_{-5}}{r^5}-\frac{\Omega_{-3}}{r^3}+\Omega_{-2}\frac{\log r}{r^2}+\frac{\Omega_{-1}}{r}$$
$$+\Omega_0+\Omega_1r+\Omega_2r^2+\Omega_3r^3+\Omega_4r^4+\Omega_5r^5+\Omega_6r^6+\Omega_7r^7+\Omega_8r^8+\Omega_{10}r^{10}, \quad (22a)$$

where ρ_2, v_2, ρ_3 and v_1 are the known functions. The symbol $\bar{\Omega}$ is an integration constant. The symbols $\Omega_{-5}, \Omega_{-3}, \ldots, \Omega_{10}$ are the coefficients in terms of M_∞, γ, and the shock configuration coefficients. They are

$$\Omega_{-5} = -\frac{\gamma-2}{128}\frac{\rho_0^2}{\gamma^2p_0^2}G^5,$$
$$\Omega_{-3} = -\frac{9}{4}\frac{\rho_0}{\gamma p_0}G^2H_1,$$
$$\ldots \qquad \ldots$$
$$\Omega_{10} = \frac{1}{2}\left[-\frac{1}{24}\frac{\rho_0}{\gamma p_0}A^2H_5+\frac{1}{96}\frac{6}{(\gamma-1)c}AJ_5+\ldots+Q_{10}\right].$$

REFERENCES

Bazzhin, A. P. & Gladkov, A. A. 1963 Some considerations on the solution of converse problems by a series-expansion method (in Russian). *Inzhenernyi Zhurnal* **3**, 517–18.

Bohachevsky, I. O., Rubin, E. L. & Mates, R. E. 1965 A direct method for computation of nonequilibrium flows with detached shock waves. *AIAA Paper* no. 65-24.

Cheng, H. K. & Gaitatzes, G. A. 1966 Use of the shock layer approximation in the inverse hypersonic blunt body problem. *AIAA J.* **4**, 406–13.

Conti, R. 1964 Stagnation equilibrium layer in nonequilibrium blunt-body flows. *AIAA J.* **2**, 2044–6.

CONTI, R. 1966 A theoretical study of nonequilibrium blunt-body flows. *J. Fluid Mech.* **24**, 65–88.

HAYES, W. D. & PROBSTEIN, R. F. 1959 *Hypersonic Flow Theory*, chaps. v and vi. New York: Academic Press.

INCE, E. L. 1926 *Ordinary Differential Equations*, chap. xii. New York: Dover.

KAO, H. C. 1965 A new technique for the direct calculation of blunt-body flow fields. *AIAA J.* **3**, 161–3.

KENDALL, J. M. 1959 Experiments on supersonic blunt-body flows. *California Institute of Technology, JPL Progress Rept.* no. 20-372.

LAX, P. D. 1954 Weak solutions of nonlinear hyperbolic equations and their numerical computations. *Communs. Pure and Appl. Math*, **7**, 159–93.

LOMAX, H. & INOUYE, M. 1964 Numerical analysis of flow properties about blunt bodies moving at supersonic speeds in an equilibrium gas. *NASA Tech. Rept.* TR-R-204.

MASLEN, S. H. 1964 Inviscid hypersonic flow past smooth symmetric bodies. *AIAA J.* **2**, 1055–61.

SWIGART, R. J. 1963 A theory of asymmetric hypersonic blunt-body flows. *AIAA J.* **1**, 1034–42.

VAN DYKE, M. D. & GORDON, H. D. 1959 Supersonic flow past a family of blunt axisymmetric bodies. *NASA Tech. Rept.* R-1.

VAN DYKE, M. D. 1964 Perturbation methods in fluid mechanics, chap. iii. New York: Academic Press.

VAN DYKE, M. D. 1965 Hypersonic flow behind a paraboloidal shock wave. *J. de Mécanique*, **4**, 4, 477–93.

VAN DYKE, M. D. 1966 The blunt-body problem revisited. *Fundamental Phenomena in Hypersonic Flow.* Ed. by J. G. Hall. Ithaca, N.Y.: Cornell University Press.

XERIKOS, J. & ANDERSON, W. A. 1965 An experimental investigation of the shock layer surrounding a sphere in supersonic flow. *AIAA J.* **3**, 451–7.